Bull. Mater. Sci. (2021) 44:166
https://doi.org/10.1007/s12034-021-02456-9

Comparison of the antifungal activity of fluconazole- and ketoconazole-loaded PCL/PVP nanofibrous mat

MEHRAN AFRASHI[1], MINA NASARI[1], DARIUSH SEMNANI[1,3,*], PARVIN DEHGHAN[2] and MEHRNOUSH MAHERONNAGHSH[2]

[1]Department of Textile Engineering, Isfahan University of Technology, 84156-83111 Isfahan, Iran
[2]Department of Parasitology and Mycology, School of Medicine, Isfahan University of Medical Sciences, Isfahan, Iran
[3]Textile Engineering Department, Amirkabir University of Technology, Tehran, Iran
*Author for correspondence (d_semnani@cc.iut.ac.ir)

MS received 26 August 2020; accepted 13 February 2021

Abstract. In this study, the antifungal activity of both fluconazole and ketoconazole was compared. The drugs were loaded into the polycaprolactone (PCL)/polyvinylpyrrolidone (PVP) nanofibrous mats and the effect of the drug-loaded samples on *Candida albicans* (*Ca*) were investigated by disc diffusion method. Furthermore, the characterization of nanofibrous mats was performed by field emission scanning electron microscopy, Fourier transform infrared (FT-IR) and contact angle tests. The mean diameter of nanofibres was 656 nm and it decreased with the addition of drugs into the electrospinning solutions, because the viscosity of solutions were decreased while electron conductivity of solutions was increased. With increase in the amount of the drug from 5 to 15%, the hydrophilicity increased. FT-IR revealed both drugs were physically embedded in the nanofibres and confirmed their presence in the composition. In addition, the degradation behaviour of samples was significant due to by the amount and the dissolution of PVP and approximately 40% loss weight occurred after 22 days. In the disc diffusion tests, both drug-loaded samples had antifungal effect on sensitive isolates of *Ca*, while for resistant of isolate the ketoconazole had more effective than fluconazole. Overall, the study highlights the ability of antifungal drug-loaded PVP/PCL nanofibrous mats as potential wound dressing materials and local delivery systems.

Keywords. Electrospinning; drug delivery systems; antifungal activity; fluconazole; ketoconazole; nanofibrous mat.

1. Introduction

Drug delivery systems (DDSs) are rapidly developing to help pharmacological effects. They promote patient comfort and reduce drug toxicity as opposed to conventional drug usage. Major progress has been made in the design of appropriate carriers with the capability of controlling the amount of drug delivery, increasing drug bioavailability and reducing the side effects [1,2]. Furthermore, the DDSs can prevent degradation of the drugs [3]. Some of the most successful DDSs were designed for local delivery [4]. New DDSs that fabricated with suitable polymers have provided many ways to enhance the effectiveness of drugs. The drug can be loaded into/onto the fibers by some methods such as coating and electrospinning to fabricate drug-loaded nanofibres [5]. They are one of the suitable choice for biomedicine like as fibrous scaffolds, wound healing, and DDSs due to their unique properties, such as high surface-to-volume ratio, highly porous and acceptable strength [6,7].

In a recent research, the nanofibres has been used for delivery of drugs with low solubility [8,9]. Furthermore, they exhibit sustained DDSs [10]. Usually, nanofibres are produced directly from most polymers by electrospinning method [11]. They are fabricated using different synthetic and/or natural polymers for biomedical applications [7]. Polycaprolactone (PCL) is one of the synthetic and approved polymers for biomedical usage. It is biocompatible and also low cost [12,13]. Furthermore, it is approved by FDA and has potentials to use for DDSs as electrospun nanofibre [14].

Polyvinylpyrrolidone (PVP) is another biocompatible synthetic polymer. It is used for biomedical applications due to some features such as water-solubility and non-toxicity [15]. PVP and PCL nanofibres are commonly used in biomaterials as blended, core-shell or multilayered [16–18]. Suganya *et al* [19] demonstrated PCL/PVP nanofibre containing a medicinal plant for wound healing and evaluated their antibacterial properties. Lee *et al* [20] prepared the effect of electrospun PCL/PVP scaffolds on stem cells. Veeren *et al* [21] reported on the successfully loading of

Published online: 03 June 2021

various anticancer drugs into the PVP/PCL nanomicelles. Li *et al* [22] developed an electro-hydrodynamic jet 3D printing of PCL/PVP composite scaffold for cell culture.

Vaginal candidiasis (VVC) is an opportunistic mucosal infection caused by yeast-like fungi localized on the female genital tract. *Candida albicans* (*Ca*) species are the most common causes of VVC. It was reported to account for 85–95% of yeast strains isolated from the lower genitourinary tract. VVC affects approximately 75% of healthy women at least once during their lifetime; and about 5–8% of them experience recurrent VVC [23–25]. VVC has some symptoms such as pain, itching, irritation, vaginal discharge, erythema and dysuria [26]. The infection is often associated mainly in the immunocompromised and/or diabetic women, and who are pregnant or the women who use high estrogen contraceptives [27,28].

The treatment of *Ca* infections is based on the administration of antifungal medications from different pharmacological classes, such as imidazoles and triazoles [29]. Triazole antifungals agents, such as ketoconazole and fluconazole are a systemic therapies for patients who require treatment against fungal infections [30,31]. The azole drugs can be used orally (tablets and capsules) or locally, such as solutions, creams, etc. [24]. However, the oral dosage forms exhibit drug interactions and can cause allergic responses and systemic toxicity. The local use of azoles is safer. Anyway, the vaginal delivery systems do not persuade the retention of the drug in the vagina [32,33].

In this study, PVP/PCL-based electrospun nanofibres were performed subsequently to load fluconazole and ketoconazole drugs. Therefore, in the study, we aim to fabricate fluconazole/PVP/PCL and ketoconazole/PVP/PCL nanofibres with superior antifungal activity and good biocompatibility by electrospinning technology. The samples were characterized by field emission scanning electron microscopy (FE-SEM), Fourier transform infrared (FT-IR) analysis and contact angle tests. After that, the antifungal effects of the samples were assayed by disc diffusion method.

2. Materials and methods

2.1 *Materials*

PCL (Mw = 70000–9000 g mol^{-1}) and PVP (Mw = 360000 g mol^{-1}) were purchased from Sigma-Aldrich. Chloroform and methanol were obtained from Merck Co. (Germany). Phosphate buffer saline (PBS) solution was obtained from Cyto Matin Gene, Iran. Fluconazole and ketoconazole were purchased from the Amin pharmaceutical Co, Iran.

2.2 *Methods*

2.2a *Preparation of the electrospinning solutions:* Two series of solutions, i.e., without drug and with drug were prepared for electrospinning. Table 1 shows the components of each electrospinning solution.

Solution without drug (sample with S1 code): To provide solution with concentration of 12% (wt/vol), PCL and PVP with a ratio of 80:20 were dissolved in chloroform/methanol solution with a ratio of 4:1. Prepared solution was stirred on magnetic stirrer for 24 h at a temperature of 25°C.

Solution with drug (samples with S2–S7 code): Fluconazole and ketoconazole were selected to be loaded in nanofibres separately. The preparation of solutions containing fluconazole and ketoconazole was similar. At first, certain amount of the drug (according to Table 1) was dissolved in methanol and the solution was stirred for 3 h, then PCL, PVP and chloroform were added to it. The amounts of these materials were as described in the previous section. These solutions were stirred for 24 h at a temperature of 25°C.

2.2b *Viscosity and electron conductivity:* The viscosity of all electrospun solutions was measured with a viscometer (Brookfield, USA). The spindle of viscometer was worked at six different speeds (0.5, 1, 2, 2.5, 4 and 5 rpm). Furthermore, a conductivity meter (Jenway, Barloword Scientific Ltd., EU) was used to measure the electron conductivity of the solutions.

2.2c *Electrospinning of nanofibres:* Electrospinning method was used to fabricate nanofibre mats. Electrospinning setup consists of a syringe pump (Pars Nanoris, Iran), fixed drum as the collector and high-voltage DC power supply (Pars Nanoris, Iran). Each of electrospinning solutions was transferred to syringe with a needle gauge of 23 and fed at constant rate 0.2 ml h^{-1}. The distance between nozzle and fixed collector drum was 18 cm. The applied voltage used for the production of nanofibres was 12 kV. Temperature and humidity were constant (25°C and 65%, respectively) during the electrospinning process.

2.3 *Characterization of nanofibres*

2.3a *FE-SEM:* Morphology of electrospun nanofibres was investigated by FE-SEM (Philips EM 208S, USA). In each FE-SEM image, 100 fibres were selected and the diameter of them were measured by using Digimizer software.

2.3b *FT-IR analysis:* FT-IR analysis was performed to confirm the presence of fluconazole and ketoconazole in nanofibres and investigation of chemical reactions between PVP, PCL and drugs. Electrospun nanofibres and pure polymers were mixed with potassium bromide (KBr) and were pressed well to form a pill. Fourier transform infrared analysis (FTIR, Victoria, Australia) was used in the range

Table 1. Components of each electrospinning solution.

Sample codes	Compound	PCL/PVP (%)	Fluconazole (%)	Ketoconazole (%)
S1	PCL/PVP	80/20	0	0
S2	PCL/PVP/5% fluconazole	80/20	5	0
S3	PCL/PVP/10% fluconazole	80/20	10	0
S4	PCL/PVP/15% fluconazole	80/20	15	0
S5	PCL/PVP/5% ketoconazole	80/20	0	5
S6	PCL/PVP/10% ketoconazole	80/20	0	10
S7	PCL/PVP/15% ketoconazole	80/20	0	15

400–4000 cm^{-1} at room temperature. OMINIC software was used for analysing FT-IR spectrum.

2.3c *Nanofibres degradation:* To determine the degradation of nanofibrous mats, loss weight method was used according to ASTM F1635-04A 31. For each time interval, three pieces (4 × 4 cm) of the sample without drug (sample with S1code) were cut and their weights were measured. Then the samples were transferred to Petri dishes contains 5 ml of PBS (pH = 7.4) at the temperature of 37°C. The samples were removed from the Petri dish and they were dried under vacuum after specified time intervals. In addition, the weight of samples was measured after drying.

Weight loss was calculated according to the following equation:

$$\text{weight loss}\% = \frac{w_1 - w_2}{w_1} \times 100\,,$$

where, w_1 was sample's weight before soaking in PBS and w_2 was sample's weight after soaking in PBS and dried.

2.3d *Hydrophobicity assessment:* The contact angle of distilled water on the surface nanofibre mats was measured to investigate the surface hydrophobicity or hydrophilicity. In this method, a drop of distilled water was dropped by micropipette on the flat surface of each sample at three different points. A digital camera (Canon, Japan) was used to take image from the sample during this process. The angle between the water droplet and surface of samples were measured from digital image by using the Digimizer software.

2.3e *In-vitro test-disk diffusion method:* The antifungal activity of the drug-loaded nanofibrous samples were carried out by disc diffusion method to determine the sensitivity of the *Ca* Pttc 5027 to ketoconazole and fluconazole, according to CLSI M44-S2 protocols. For this purpose, a suspension of the Candida with concentration of 0.5 MacFarland standards was prepared and then it was spread on a plate containing Sabouraud dextrose agar (Merck, Germany) with a sterile swab. After that 6 mm disk shapes of the samples containing different amount of the drugs were prepared and they were put on the prepared plates. Then, the inoculated plates were incubated at 37°C for 24 h and the diameter of the inhibited haloes around the disks were measured and expressed in millimetres as its antifungal property [34].

3. Results and discussion

3.1 *Viscosity and electron conductivity*

Viscosity and electron conductivity are two influential factors in the electrospinning process. For example, if both viscosity and electron conductivity are low, the electrospray process takes place instead of electrospinning, resulting in nanoparticles. Table 2 presents the results of viscosity test. According to the table, the viscosity of each sample was decreased with increase in the speed of spindle from 0.5 to 5 rpm. Furthermore, the viscosity of the solutions was decreased with addition of fluconazole and ketoconazole to PCL/PVP solution and increasing their quantity.

The results of electron conductivity are shown in table 3. The Conductivity of the solutions was increased by adding fluconazole and ketoconazole to the PCL/PVP solutions. In addition, it was increased with increase in the concentration of drugs.

3.2 *Morphology of nanofibres*

Figure 1a–g shows FE-SEM images of PCL/PVP nanofibrous mats with and without fluconazole and ketoconazole. All of the samples were uniform and beedless. Table 4 shows the results of measuring the diameter of the nanofibres diameter by Digimizer software.

Figure 1h indicates the average fibre diameter of the sample loaded with fluconazole compared to similar blank sample. The mean diameter of PCL/PVP nanofibres was 656 ± 179 nm, which decreased to 577 ± 226, 467 ± 96 and 439 ± 137 nm by adding 5, 10 and 15% wt fluconazole, respectively. In addition, according to figure 1i, the mean diameter of PCL/PVP nanofibres was 656 ± 179 nm, which

Table 2. Viscosity of electrospinning solutions.

Sample codes	Viscosity (cP)					
	RPM = 0.5	RPM = 1	RPM = 2	RPM = 2.5	RPM = 4	RPM = 5
S1	1269.95	536.00	515.50	430.00	412.00	404.00
S2	1257.00	524.45	378.95	353.55	335.95	326.65
S3	881.00	424.50	368.00	329.50	280.45	264.65
S4	723.20	410.15	356.23	320.00	274.20	256.00
S5	1229.50	525.40	508.15	429.40	407.25	400.90
S6	943.55	504.90	500.95	419.70	392.35	364.40
S7	893.95	382.95	356.70	345.65	308.05	281.80

Table 3. Electron conductivity of electrospinning solutions.

Sample codes	Electron conductivity (μs)
S1	1.38 ± 0.75
S2	2.25 ± 0.18
S3	7.22 ± 0.32
S4	9.56 ± 0.29
S5	6.31 ± 2.10
S6	7.56 ± 0.26
S7	10.47 ± 0.54

decreased to 564 ± 165, 505 ± 196 and 416 ± 130 nm by adding 5, 10 and 15% wt ketoconazole, respectively.

This reduction in diameter can be attributed to the thinning of the jet during the electrospinning process [35]. As the dose of drug was increased, the fibres pull harder towards the collector and take on the shape of a horned horn due to the instability of the electrospinning jet. Another reason for the decrease in diameter with the addition of the drug can be attributed to the increase in conductivity and decrease in viscosity [36]. According to the results of viscosity measurement, PCL/PVP solution viscosity (all mentioned speed of spindle) was decreased after adding both of the drugs (fluconazole and ketoconazole). Furthermore, it was decreased with increase in amount of the drugs from 5 to 15%. Unlike of the viscosity, the electron conductivity was increased with the addition of drugs and increase in their quantity. These parameters can have an effect on the nanofibres diameter and they were decreased with adding the drugs and increasing their concentrations.

No beaded fibres were found in FE-SEM images after loading fluconazole and ketoconazole in nanofibres with various amounts.

3.3 *FT-IR analysis*

FT-IR analysis was performed to investigate the functional groups of compounds and chemical interactions between them.The FT-IR spectra of PCL, PVP and PCL/PVP are shown in figure 2a.

In PCL spectra, vibration of C=O (carboxyl group which is ester functional group) and C–O were located at 1720 and 1175 cm^{-1}, respectively [37–39]. In PVP spectra, vibration of C=O (in amide) and C–N were found at 1662 and 1423 cm^{-1}, respectively [38,39]. A broad peak at 3230–3550 cm^{-1} is related to O–H bond [40]. The PVP and PCL index peaks were also observed in the blend PCL/PVP nanofibres, indicating the presence of these two polymers in the composition [41]. In addition, no change was observed in the peak at position 2939 cm^{-1}. This peak belongs to the alkanes group that forms the polymer backbone [38].

Figure 2b illustrates fluconazole, ketoconazole, PCL/PVP/fluconazole and PCL/PVP/ketoconazole FT-IR spectra. In fluconazole spectra, vibration of triazole ring was found at 1508 and 1420 cm^{-1}. Two peaks located at 1618 and 1017 cm^{-1} were related to stretching bond of C=C and stretching C–(OH). In addition, stretching of CF groups was found at 1277 cm^{-1}. Peaks in the region 1650–1760 cm^{-1} were related to (C(=O)OH)(carboxyl group) [42–44].

In ketoconazole spectra, stretching vibration of C=O (carbonyl group), aromatic stretching C=C and stretching of cyclic C–O (ether) exhibited at 1743 and 1645 cm^{-1}, 1505 and 1240 cm^{-1}, respectively [45,46]. Stretching of N–H and C–Cl was observed at 3085 and 814 cm^{-1}. Stretching of C–H (aliphatic) was observed at 2927 and 2740 cm^{-1} [47]. Two peaks which appeared at 1223 and 1200 cm^{-1} are related to tertiary (3°) amine [48]. Index peaks of PVP, PCL, fluconazole and ketoconazole were found in PCL/PVP/fluconazole and PCL/PVP/ketoconazole spectra, which confirmed the presence in the composition. No changes were observed in other peaks.

3.4 *Nanofibres degradation*

Figure 3 illustrates the weight loss of PCL/PVP nanofibrous mats during 528 h.

PCL is synthetic biomaterial with hydrophobic nature. This polymer has no functional group in its structure, also degraded over a long period of time (3–5 years) [49]. PVP is a water-soluble polymer with excellent biocompatibility and low cytotoxicity [50]. A suitable scaffold with

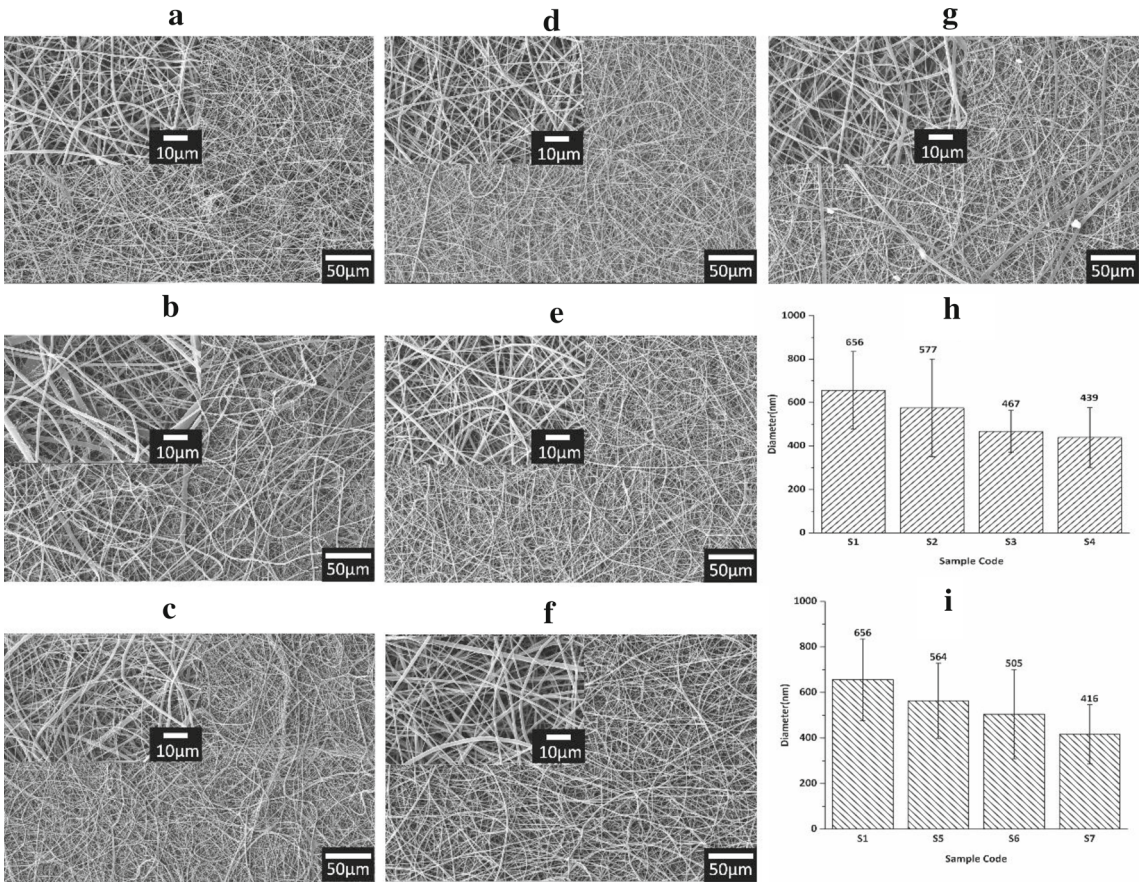

Figure 1. (**a**–**g**) FE-SEM images of S1, S2, S3, S4, S5, S6 and S7 and (**h** and **i**) the average fibre diameter of sample loaded with fluconazole and ketoconazole compared with similar blank, respectively.

Table 4. Results of measuring the nanofibre's diameter.

Sample codes	PCL/PVP (%)	Fluconazole (%)	Ketoconazole (%)	Nanofibre diameter (nm)
S1	80/20	0	0	656 ± 179
S2	80/20	5	0	577 ± 226
S3	80/20	10	0	467 ± 96
S4	80/20	15	0	439 ± 137
S5	80/20	0	5	564 ± 165
S6	80/20	0	10	505 ± 196
S7	80/20	0	15	416 ± 130

hydrophilicity and desirable degradation properties are obtained by blending PCL with PVP [51]. According to previous studies, adding PVP to PCL improves its hydrophilicity. The porosity of PCL/PVP nanofibres mat was increased after degradation due to the dissolution of PVP in the PBS solution [41] and contact with surrounding environment increased [40]. The degradation in the first 7 days (168 h) was very significant due to the dissolution of PVP [51]. Approximately 40% weight loss occurred after 22 days.

3.5 *Contact angle measurements*

The contact angle measurements result of all samples are presented in figure 4 and table 5.

PCL is widely used in medical applications, while it is hydrophobic and there are no functional groups on its surface [52]. Hydrophilicity of PCL improved by adding PVP to it [53] due to hydrophilicity of the PVP [41], which leads to the formation of hydrogen bond between PVP and water molecules. PCL/PVP nanofibres become more hydrophilic

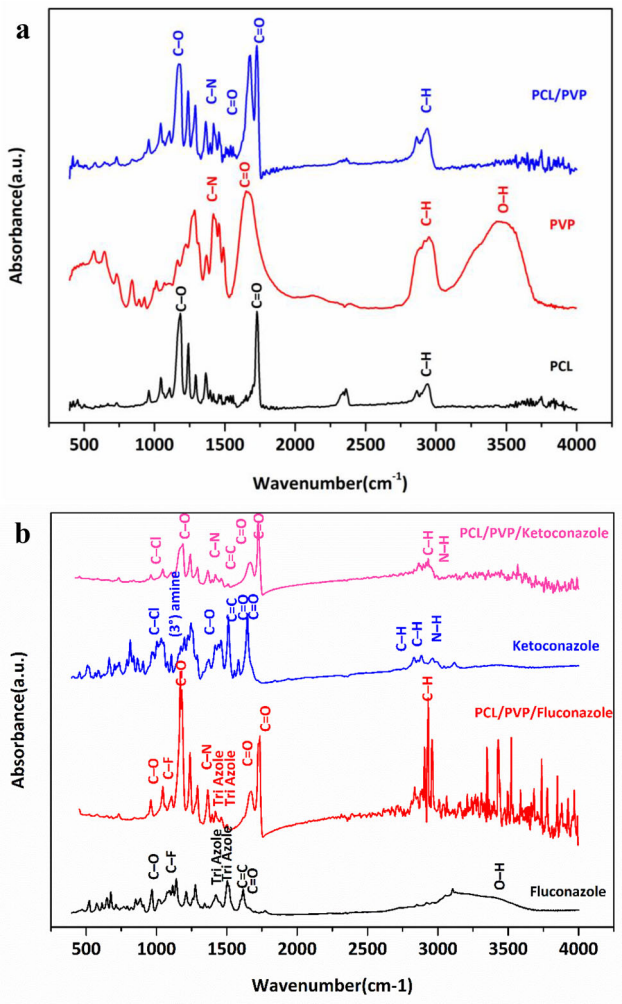

Figure 2. FTIR spectra of (**a**) PCL, PVP and PCL/PVP nanofibrous mats and (**b**) fluconazole, ketoconazole and both of drug loaded into PVP/PCL nanofibres.

by the addition of fluconazole and ketoconazole. In addition, with increase in the amount of the drug from 5 to 10 and 15%, the contact angle decreased and hydrophilicity increased. Adding the drug may smooth the surface of nanofibres, which helps hydrophilicity [54]. On the other hand, result of fibre diameters shows reduction after adding drug; therefore, hydrophilicity was increased by reduction of fibre diameter and increase in surface area [55].

3.6 *In-vitro test-disk diffusion method*

Figure 5 shows the results of the disc diffusion tests. Furthermore, the diameters of the inhibited zones around the disks are presented in table 6.

Candida is a common human fungal pathogen which is capable of causing local infections. More than a billion people worldwide travail from fungal infections, and recently, these infections has significantly increased due to a rise in the number of immunocompromised patients. On the other hand, antifungal resistance has increased due to reasons like the lack of compliance of patients and the decrease in release rate of new antifungal drugs [56].

In this study, it was demonstrated that the fluconazole- and ketoconazole-loaded nanofibrous mats had inhibitory effects against resistant and sensitive *Ca*. If the diameter of inhibition zone around the isolate is more than 19 mm, the isolate is sensitive to the drugs (19 S) and if the diameter is fewer than 14 mm, the isolate is considered resistant to them (6 R) [57]. According to the disc diffusion tests and for the resistant isolates, the inhibition zones for the concentrations of 5, 10 and 15% ketoconazole-loaded mats were determined 2, 5 and 7 mm, respectively. While for the sensitive isolates, they are 12, 15 and 17 mm, respectively. The growth inhibition zone of fungal around the disks

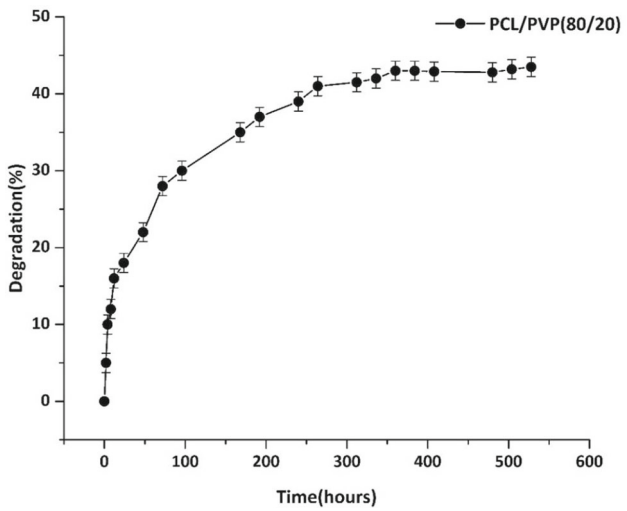

Figure 3. Weight loss of PCL/PVP nanofibrous mats.

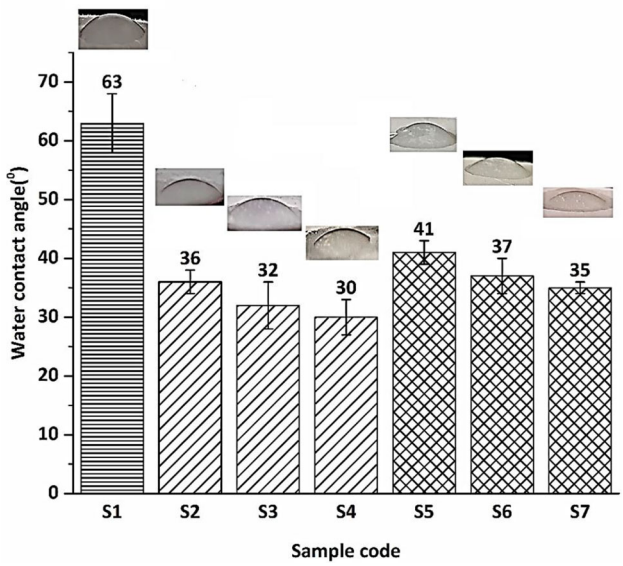

Figure 4. The contact angle measurements.

Table 5. The contact angle measurements of all samples.

Sample codes	PCL/PVP (%)	Fluconazole (%)	Ketoconazole (%)	Water contact angle (°)
S1	80/20	0	0	63 ± 5
S2	80/20	5	0	36 ± 2
S3	80/20	10	0	32 ± 4
S4	80/20	15	0	30 ± 3
S5	80/20	0	5	41 ± 2
S6	80/20	0	10	37 ± 3
S7	80/20	0	15	35 ± 1

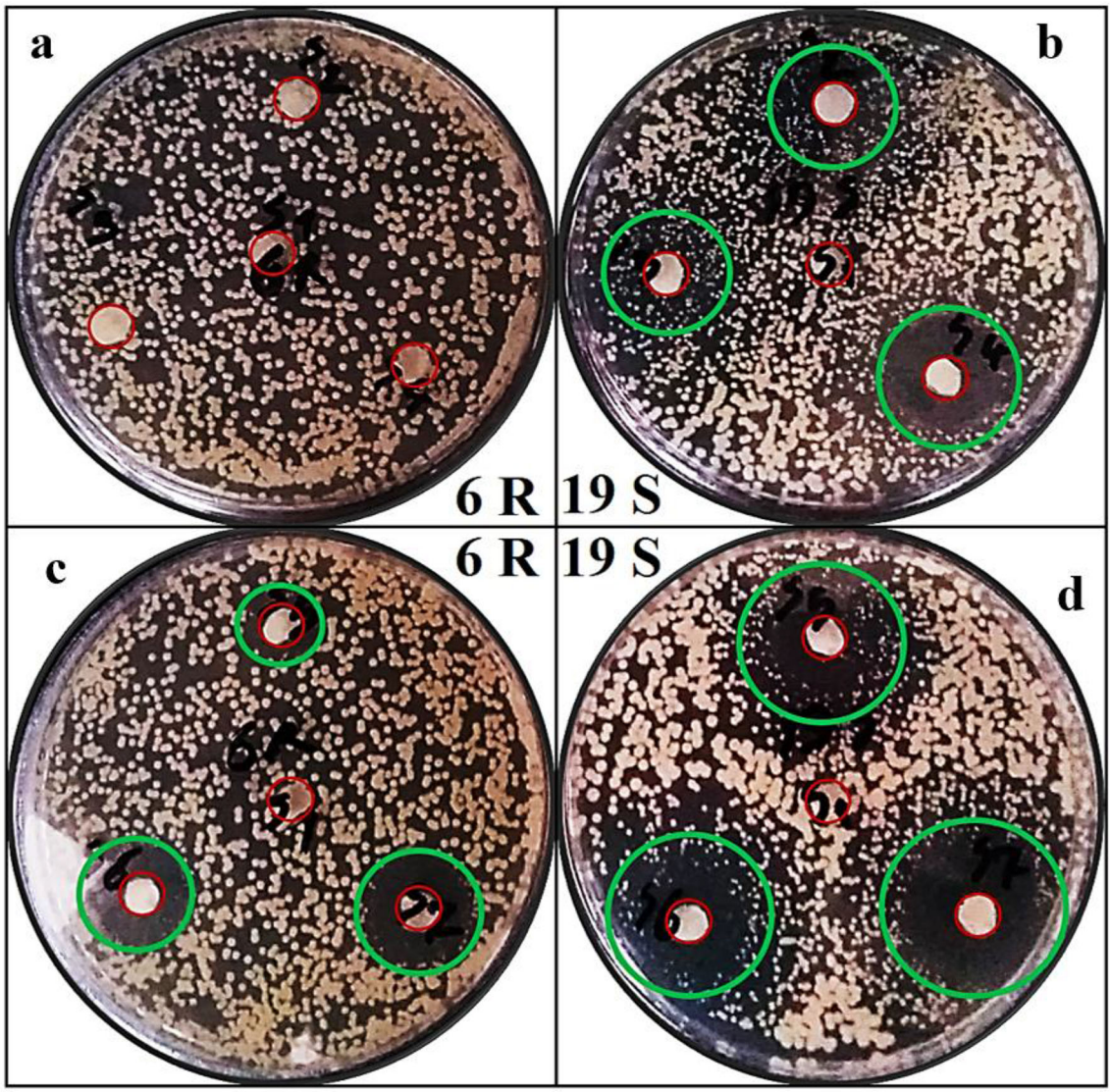

Figure 5. Antifungal activities of (**a** and **b**) fluconazole and (**c** and **d**) ketoconazole-loaded PCL/PVP nanofibrous mat.

shows that these samples have a good ability to ketoconazole release and eliminating fungal. Furthermore, for the sensitive isolates, the diameters of growth inhibition zone of the fluconazole samples (5, 10 and 15%) were between 7 and 10 mm and they can prevent the growth of the fungal around the fluconazole-loaded samples. However, different concentrations of the fluconazole-loaded samples do not have antifungal effect on resistant isolates of *Ca*.

Table 6. Zone of inhibition of drug-loaded disks in *CA*.

	6 R							19 S						
Samples	S1	S2	S3	S4	S5	S6	S7	S1	S2	S3	S4	S5	S6	S7
Zone of inhibition in *Ca* (mm)	0	0	0	0	2	5	7	0	7	8	10	12	15	17

4. Conclusion

PCL/PVP nanofibrous mats with and without fluconazole and ketoconazole were successfully prepared by electrospinning. FE-SEM and contact angle test showed that the nanofibres had the uniform morphology and hydrophilic surface, respectively. The hydrophilicity of the samples was increased by increasing the drug amounts due to the effect of drugs on surface smoothing and increasing the surface area. In addition, FT-IR results showed that PCL/PVP nanofibrous mats were successfully loaded with fluconazole and ketoconazole. In addition, the drug-loaded samples had good antifungal effect for *Ca*, while ketoconazole-loaded samples had more effective than the fluconazole ones, especially for resistant isolates. The results showed that both the drug-loaded samples had effective antifungal properties and can be used for local drug delivery.

References

[1] Uhrich K E, Cannizzaro S M, Langer R S and Shakesheff K M 1999 *Chem. Rev.* **99** 3181

[2] Tamizi E, Azizi M, Seyed Dorraji M S, Dusti Z and Panahi-Azar V 2018 *Polym. Bull.* **75** 547

[3] Hadjianfar M, Semnani D and Varshosaz J 2018 *Polym. Adv. Technol.* **29** 2972

[4] Weiser J R and Saltzman W M 2014 *J. Control Release* **28** 664

[5] Kaviannasab E, Semnani D, Khorasani S N, Varshosaz J, Khalili S and Ghahreman F 2019 *Mater. Res. Express.* **61** 15015

[6] Bhandari J, Mishra H, Mishra P K, Wimmer R, Ahmad F J and Talegaonkar S 2017 *Int. J. Nanomed.* **7** 2021

[7] Shadamarshan R P, Balaji H, Rao H S, Balagangadharan K, Chandran S V and Selvamurugan N 2018 *Colloids Surf. B Biointerfaces* **171** 698

[8] Golchin A, Hosseinzadeh S and Roshangar L 2018 *Med. Mol. Morphol.* **51** 1

[9] Shitole A A, Giram P S, Raut P W, Rade P P, Khandwekar A P, Sharma N and Garnaik B 2019 *J. Biomater. Appl.* **33** 1327

[10] Shitole A A, Raut P, Giram P, Rade P, Khandwekar A, Garnaik B *et al* 2020 *Mater. Sci. Eng. C* **110** 110731

[11] Golchin A, Hosseinzadeh S, Staji M, Soleimani M, Ardeshirylajimi A and Khojasteh A 2019 *J. Cell Biochem.* **120** 15410

[12] Perumal G, Sivakumar P M, Nandkumar A M and Doble M 2020 *Mater. Sci. Eng. C* **109** 110527

[13] Fadaie M, Mirzaei E, Geramizadeh B and Asvar Z 2018 *Carbohydr. Polym.* **199** 628

[14] Zupančič Š, Preem L, Kristl J, Putrinš M, Tenson T, Kocbek P *et al* 2018 *Eur. J. Pharm. Sci.* **122** 347

[15] Kumar R, Rai B and Kumar G 2019 *J. Polym. Environ.* **27** 2963

[16] Li R, Cheng Z, Yu X, Wang S, Han Z and Kang L 2019 *Mater. Lett.* **254** 206

[17] Zhu L F, Zheng Y, Fan J, Yao Y, Ahmad Z and Chang M W 2019 *Eur. J. Pharm. Sci.* **137** 105002

[18] Kim G, Park J and Park S 2007 *J. Polym. Sci. Part B Polym. Phys.* **45** 2038

[19] Suganya S, Senthil Ram T, Lakshmi B S and Giridev V R 2011 *J. Appl. Polym. Sci.* **121** 2893

[20] Lee Y J, Elosegui-Artola A, Le K H T and Kim G M 2013 *Cell. Mol. Bioeng.* **6** 482

[21] Veeren A, Bhaw-Luximon A, Mukhopadhyay D and Jhurry D 2017 *Eur. J. Pharm. Sci.* **102** 250

[22] Li K, Wang D, Zhao K, Song K and Liang J 2020 *Talanta* **211** 120750

[23] Jang S J, Lee K, Kwon B, You H J and Ko G P 2019 *Sci. Rep.* **9** 1

[24] Melo C M, Cardoso J F, Perassoli F B, de Oliveira Neto A S, Pinto L M, de Freitas Marques M B *et al* 2020 *Carbohydr. Polym.* **230** 115608

[25] Sun X, Gao Y, Ding Z, Zhao Y, Yang Y, Sun Q *et al* 2020 *Int. J. Biol. Macromol.* **148** 1053

[26] Kenechukwu F and Attama A 2018 *BioMed. Res. Int.* **2018** 3714329

[27] Bignoumba M, Onanga R, Mboumba B B, Gafou A, Ndzime Y M, Lendamba R W *et al* 2019 *J. Mycol. Med.* **29** 317

[28] Sobel J D 2016 *Am. J. Obst. Gynecol.* **214** 15

[29] Souza R O, de Lima T H, Oréfice R L, de Freitas Araújo M G, de Lima Moura S A, Magalhães J T *et al* 2018 *J. Pharm. Sci.* **107** 2674

[30] Adis Medical Writers 2020 *Drugs Ther. Perspect.* **36** 112

[31] Chen M, Zhang X, Chen Y, Sun W, Wang Z, Huang C *et al* 2020 *Xenobiotica* **50** 280

[32] Calvo N L, Svetaz L A, Alvarez V A, Quiroga A D, Lamas M C and Leonardi D 2019 *Int. J. Pharm.* **556** 181

[33] Wang J L, Chang C H, Young-Xu Y and Chan K A 2010 *Antimicrob. Agents Chemother.* **54** 2409

[34] Semnani D, Afrashi M, Alihosseini F, Dehghan P and Maherolnaghsh M 2017 *J. Mater. Sci. Mater. Med.* **28** 1

[35] Kim G M, Le K H T, Giannitelli S M, Lee Y J, Rainer A and Trombetta M 2013 *J. Mater. Sci. Mater. Med.* **24** 1425

[36] Zamani M, Morshed M, Varshosaz J and Jannesari M 2010 *Eur. J. Pharm. Biopharm.* **75** 179

[37] Han J, Branford-White C J and Zhu L M 2010 *Carbohydr. Polym.* **79** 214

[38] Álvarez-Suárez A S, Dastager S G, Bogdanchikova N, Grande D, Pestryakov A, García-Ramos J C *et al* 2020 *Micromachines* **11** 441

[39] Bai J, Li Y, Zhang C, Liang X and Yang Q 2008 *Colloids Surfaces A Physicochem. Eng. Asp.* **329** 165
[40] Nasari M, Semnani D, Hadjianfar M and Amanpour S 2020 *J. Mater. Sci.* **55** 10185
[41] Jia Y, Huang G, Dong F, Liu Q and Nie W 2016 *Polym. Compos.* **37** 2847
[42] Salerno C, Carlucci A M, Chiappetta D A and Bregni C 2011 *Latin Am. J. Pharm.* **30** 1406
[43] Afrashi M, Semnani D, Talebi Z, Dehghan P and Maherolnaghsh M 2019 *J. Non-Cryst. Solids* **503–504** 186
[44] Alkhamis K A, Obaidat A A and Nuseirat A F 2002 *Pharm. Dev. Technol.* **7** 491
[45] Veras F F, Roggia I, Pranke P, Pereira C N and Brandelli A 2016 *Eur. J. Pharm. Sci.* **84** 70
[46] Kumara P, Mohanb C, Uma Shankara M K S and Gulatia M 2011 *Iran. J. Pharm. Res.* **10** 685
[47] Papneja P, Kataria M K and Bilandi A 2015 *Eur. J. Pharm. Med. Res.* **2** 990
[48] Karolewicz B, Górniak A, Owczarek A, Zurawska-Płaksej E, Piwowar A and Pluta J 2014 *J. Therm. Anal. Calorim.* **115** 2487
[49] Lanza R, Langer R, Vacanti J and Atala A 2020 *Principles of tissue engineering* (Cambridge: Academic Press)
[50] Chung T W, Cho K Y, Lee H C, Nah J W, Yeo J H, Akaike T *et al* 2004 *Polymer (Guildf)* **45** 1591
[51] Jia Y T, Zhu X Y and Liu Q Q 2011 *Adv. Mater. Res.* **332** 1330
[52] Xue J, He M, Liu H, Niu Y, Crawford A, Coates P D *et al* 2014 *Biomaterials* **35** 9395
[53] Wang J H, Cheng X B, Huang G, Dong F C and Jia Y T 2011 *Adv. Materials Res.* **311** 1638
[54] Wang B, Chen X, Ahmad Z, Huang J and Chang M W 2019 *Carbon N Y* **153** 285
[55] Nadim A, Khorasani S M, Kharaziha M and Davoodi S M 2017 *Mater. Sci. Eng. C* **78** 47
[56] Shalini S S, Sudha V, Menaka R, Anbu N and Sivaraman D 2019 *Int. J. Trans. Res. Ind. Med.* **1** 49
[57] Wayne P 2011 *Inform. Suppl.* **31** 100